

# Some notes on perturbative stability

Alexey A. Vladimirov & Co

## I. DEFINITION

This is copy-paste from [IS& AV,1706.01473].

See references and refereed equations within it.

In the construction of the cross section, one finds several sources of perturbative uncertainties. The size of these uncertainties can be estimated by the variation of associated scales. We list here the ones that we have considered in the present work.

- *Uncertainty associated with the perturbative matching of rapidity anomalous dimension* : This uncertainty arises from the dependence (at the fixed perturbative order) on  $\mu_0$ , which should be compensated between the Sudakov factor and the boundary term  $\mathcal{D}(\mu_0)$  in the TMD evolution factor eq. (??). This uncertainty can be tested by changing  $\mu_0 \rightarrow c_1\mu_0$  and varying  $c_1 \in [0.5, 2]$ .
- *Uncertainty associated with the hard factorization scale*: This uncertainty arises from the dependence (at the fixed perturbative order) on the scale  $\mu_f (\sim Q)$  which is to be compensated between the hard coefficient function  $|C_V|^2$  and the TMD evolution factor. This uncertainty can be tested by changing  $\mu_f \rightarrow c_2\mu_f$  and varying  $c_2 \in [0.5, 2]$ .
- *Uncertainty associated with the TMD evolution factor*: This uncertainty arises from the dependence (at the fixed perturbative order) on initial scale of TMD evolution  $\mu_i$ , which is to be compensated between the evolution integral and the  $\mu$ -dependence of  $\zeta_i$  in eq. (??). This uncertainty can be tested by changing  $\mu_i \rightarrow c_3\mu_i$  and varying  $c_3 \in [0.5, 2]$ .
- *Uncertainty associated with the small- $b$  matching*: This uncertainty arises from the dependence (at the fixed perturbative order) on the scale of the small- $b$  matching  $\mu_{\text{OPE}}$  which is to be compensated between the small- $b$  coefficient function  $C_{f \leftarrow f'}$  and evolution of PDF. This uncertainty can be tested by changing  $\mu_{\text{OPE}} \rightarrow c_4\mu_{\text{OPE}}$  and varying  $c_4 \in [0.5, 2]$ .

We remark that our definition of perturbative uncertainties  $c_{1,2}$  is commonly used in the literature (as far as it can be compared among different schemes of calculation), see e.g. [? ?]. The uncertainties  $c_{3,4}$  are usually non distinguished and they are commonly varied simultaneously i.e. in the literature one finds discussions of errors for the case  $c_4 = c_3$ . To our best knowledge, the distinction of the matching and evolution uncertainties is made here for the first time.

In this way, the general expression for the cross-section in eq. (??) with our choice of scales reads

$$\begin{aligned} \frac{d\sigma}{dQ^2 dy d(q_T^2)} &= \frac{4\pi}{3N_c} \frac{\mathcal{P}}{sQ^2} \sum_{GG'} z_{ll'}^{GG'}(q) \sum_{ff'} z_{ff'}^{GG'} \\ &\times \int \frac{d^2\mathbf{b}}{4\pi} e^{i(\mathbf{b}\mathbf{q})} |C_V(Q, c_2Q)|^2 \left\{ R^f[\mathbf{b}; (c_2Q, Q^2) \rightarrow (c_3\mu_i, \zeta_{c_3\mu_i}); c_1\mu_i] \right\}^2 \\ &\times F_{f \leftarrow h_1}(x, \mathbf{b}; c_4\mu_{\text{OPE}}, \zeta_{c_4\mu_{\text{OPE}}}) F_{f' \leftarrow h_2}(x, \mathbf{b}; c_4\mu_{\text{OPE}}, \zeta_{c_4\mu_{\text{OPE}}}), \end{aligned} \quad (1.1)$$

where the evolution factor  $R$  is given in eq. (??) and the explicit expression for the  $\zeta_\mu$  is given in eq. (??). The low-normalization point  $\mu_i$  and the scale of small- $b$  operator product expansion  $\mu_{\text{OPE}}$  are fixed at the same point (??)

$$\mu_i = \mu_{\text{OPE}} = \frac{C_0}{b} + 2 \text{ GeV}. \quad (1.2)$$

The central value of the constants  $c_{1,2,3,4}$  is 1 and they are varied in order to estimate the theoretical uncertainties in the usual range (0.5, 2).

The perturbative orders of each constituent are to be combined consistently. Having at our disposal the NNLO expressions for coefficient function and N<sup>3</sup>LO expressions for anomalous dimensions, we can define four successive

Name	$ C_V ^2$	$C_{f \leftarrow f'}$	$\Gamma$	$\gamma_V$	$\mathcal{D}$	PDF set	$a_s(\text{run})$	$\zeta_\mu$
NLL/LO	$a_s^0$	$a_s^0$	$a_s^2$	$a_s^1$	$a_s^2$	nlo	nlo	NLL
NLL/NLO	$a_s^1$	$a_s^1$	$a_s^2$	$a_s^1$	$a_s^2$	nlo	nlo	NLO
NNLL/NLO	$a_s^1$	$a_s^1$	$a_s^3$	$a_s^2$	$a_s^3$	nlo	nlo	NNLL
NNLL/NNLO	$a_s^2$	$a_s^2$	$a_s^3$	$a_s^2$	$a_s^3$	nnlo	nnlo	NNLO

TABLE I: The perturbative orders studied in the fit. For each order we indicate the power of  $a_s$  of each piece that enters in the TMDs. Note, that the order of  $a_s$  and PDF set are related, since the values of  $a_s$  are taken from the PDF set.

self-contained sets of ordering. This is reported in table I. In our definition of orders we use the following logic: (i) The order of the  $a_s$ -running should be the same as the order of PDF set, since their extraction are correlated. (ii) The order of  $\mathcal{D}$  should be the same as the order of  $\Gamma$  since they enter the evolution kernel  $R$  with the same counting of logarithms (i.e.  $a_s^n \ln^{n+1} \mu$ ), and one-order higher than the order of  $\gamma_V$ , since it has counting  $a_s^n \ln^n \mu$ . (iii) The order of small- $b$  matching coefficient should be the same as the order of evolution of a PDF, because large logarithms of  $b$  are to be compensated by the PDF evolution. (iv) The order of  $\zeta_\mu$  should be such that no logarithms appear in the coefficient function, and the general logarithm counting coincides with the counting of the evolution factor. In table I the order of the  $\zeta_\mu$  is defined as following: NLL is  $\mathbf{1}_\zeta = \mathbf{L}_\mu/2$ , NLO has in addition finite part at order  $a_s^0$  (i.e. two first terms of eq. (??)), NNLL has in addition logarithmic part at order  $a_s^1$  (i.e. the first line of eq. (??)), and NNLO is given by whole expression eq. (??).

To label the orders we use the nomenclature where the part with 'LO suffix designates the order of coefficient functions, and the part with 'LL suffix designates the order of the evolution factor in the  $a_s \ln \mu \sim 1$  scheme. So, our highest order is NNLL/NNLO, which at the moment the highest available combination of the perturbative series.

End of copy-paste.

In the following in order to estimate the perturbative uncertainty consider variations  $\Delta_i$  such that  $c_i \in [0.5, 2], c_{i \neq j} = 1$ . I find the maximum and minimum deviation from the central value ( $c_i = 1$ )

$$\Delta\sigma_{\max} = \frac{\max\{d\sigma(\Delta_i)\}}{d\sigma(\text{central})}, \quad \Delta\sigma_{\min} = \frac{\min\{d\sigma(\Delta_i)\}}{d\sigma(\text{central})}. \quad (1.3)$$

Naturally,  $\Delta\sigma$  depends on  $(x_{A,B}, Q, p_T)$  for Drell-Yan and  $(x, z, Q$  and  $p_T)$  for SIDIS, and on the values of  $f_{NP}$ . We fix the following

- $\Delta\sigma$  strongly depends on  $p_T$ , see [1706.01473] for multiple plots. It has some plateau in the vicinity of peak of cross-section, and grows in both direction  $p_T \rightarrow 0$  and  $p_T \rightarrow Q$ . The  $p_T \rightarrow Q$  growing is typically started at  $p_T \sim 0.25Q$  and is beyond TMD factorization region. The region and amount of growing at  $p_T \rightarrow 0$  is dependent on energy, for obvious reasons. **To set some estimator for error, we choose  $p_T$  at the peak of cross-section, i.e. at the maximum of  $p_T d\sigma/dp_T$  (central value).**
- The value of uncertainty should not strongly depend on the  $f_{NP}$ , as far as, it roughly represents the data. (However, for faster asymptotic error could be a bit slower). However, note that the position of the peak is dependent on  $f_{NP}$  which induce extra dependence. For Drell-Yan we use the functions  $f_{NP}$  from the fit [1706.01473] (model 1). **For SIDIS we use the same input as for Drell-Yan, since there is no yet fit for this data.**
- Naturally, there is dependence on the process. However, it is not essential for general picture. For Drell-Yan type of process we set  $p + \bar{p} \rightarrow Z/\gamma^* + X$  (without fiducial cuts). For SIDIS we set  $p + \gamma^* \rightarrow p^+ + X$  (without fiducial cuts).
- We took the exact differential cross-section (i.e. no kinematic integrations).

The following notes could be interesting

- The  $p_T \rightarrow 0$  growing is due to large logarithms of  $b$  at  $b \rightarrow \infty$ . **IMPORTANT NOTE:**  $\zeta$ -prescription is specially tuned to minimize/eliminate these logarithms, and thus growing is not significant (especially in the lower-energy). In other schemes, this could represent serious problem, due to uncompensated double-logarithms in the PT-tail of TMD evolution. In fact, I expect (I also checked it but it was year ago, so could not guaranty) that in non- $\zeta$ -prescriptions, the PT uncertainty  $c_{3,4}$  could grow with the increase of the order. At least I guaranty, that in non- $\zeta$ -prescriptions, PT uncertainty would not go down as fast as in  $\zeta$ -prescription.

- The experimental data is always integrated over kinematics, which smooths the uncertainties.
- The selection of  $\mu$ 's does not significantly change the uncertainty band (by definition). However, in the asymptotic regimes (especially  $b \rightarrow \infty$ ) there could be strong dependence, because  $c_i\mu$  could be very close to Landau pole. E.g. in (1.2) we specially set  $Q_0 = 2$  GeV, to ensure that it does not enter "close-to-Landau-pole" region during variations.
- I did not evaluate the value of the peak precisely but within  $\pm 1 - 2\%$ . Therefore, some funny numerical artifacts could appear.
- The constants  $c_3$  and  $c_4$  are often not distinguished. Also there is possibility to distinguish  $c_3$  and  $c_4$  within separate TMDs, which we do not use.

There are following errors in the implementation

- **The main error comes from the absence of the fit for SIDIS. Thus the peak position is determined using wrong  $f_{NP}$  and could be easily off the data completely.** But I hope that the general picture is clear.
- The PDFs and FFs (and  $\alpha_s$ ) must be taken at appropriate evolution order to make possible perturbative cancellations. However, there is no LO sets for PDFs, which is not a problem since main error at LO comes from  $c_2$ ). For FF the situation is worse. I use DSS15 input, which is at NLO only.
- While the Drell-Yan part of the `arTeMiDe` has been tested very well, the SIDIS part has not been tested so well. Thus, there are possible bugs in the code. I am working on it.
- There is a hidden error in the implementation of  $\zeta$ -prescription at NNLO (related to non-analytical behavior of evolution field at certain points). However, it is important only at high energy and (I hope) could not give significant effect (but it could reduce by error band by  $\sim 1\%$  at Z-boson). I will fix it eventually. It requires some calculations.

REMEMBER:  $\Delta\sigma$  depends on  $p_T$ . The value at peak can be affected by some accidental numerics and by  $f_{NP}$ . Thus the plot presented below should not be considered as an absolute criterion. However, in common, it gives a taste of what-is-going-on. Probably, some integrated characteristic is better.

## II. DRELL-YAN

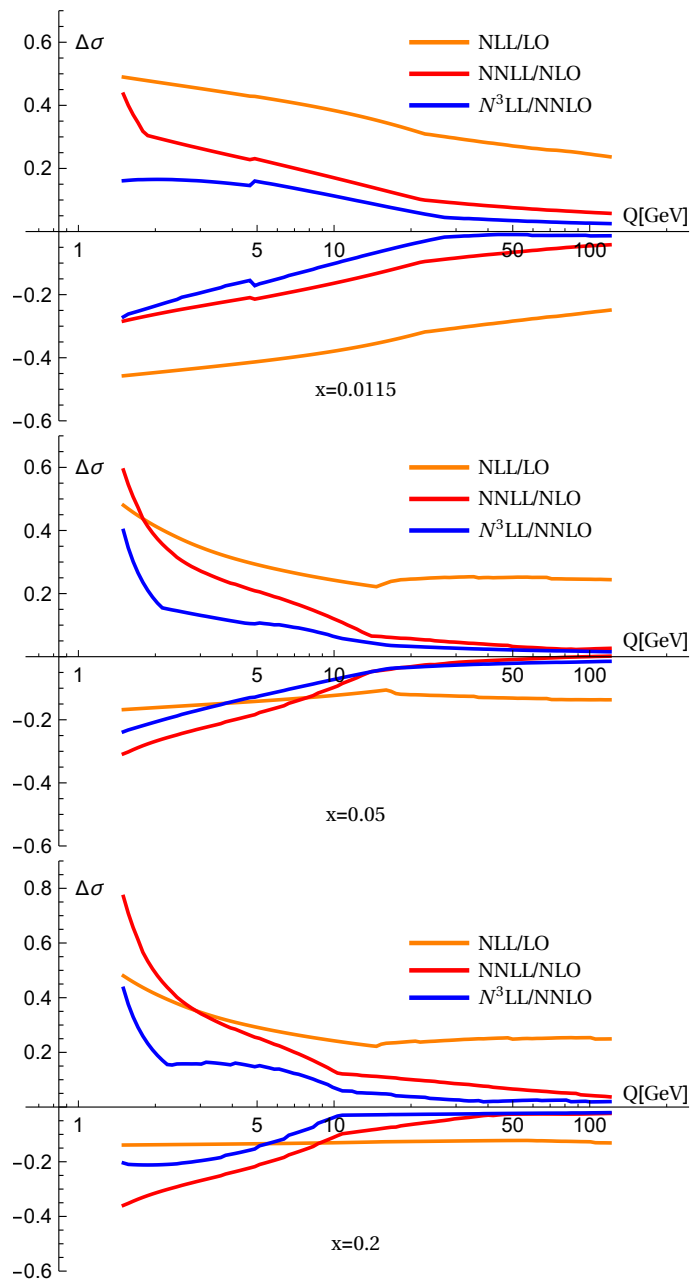


FIG. 1:  $\Delta\sigma$  for Drell-Yan process at fixed  $x$  and fixed  $y = 0$  and different values of  $Q$ .  $x = 0.0115$  roughly corresponds to LHC kinematics at Z-boson peak.  $x = 0.05$  roughly corresponds to TeVatron kinematics at Z-boson peak.  $x = 0.2$  typical  $x$  for E288 experiment.

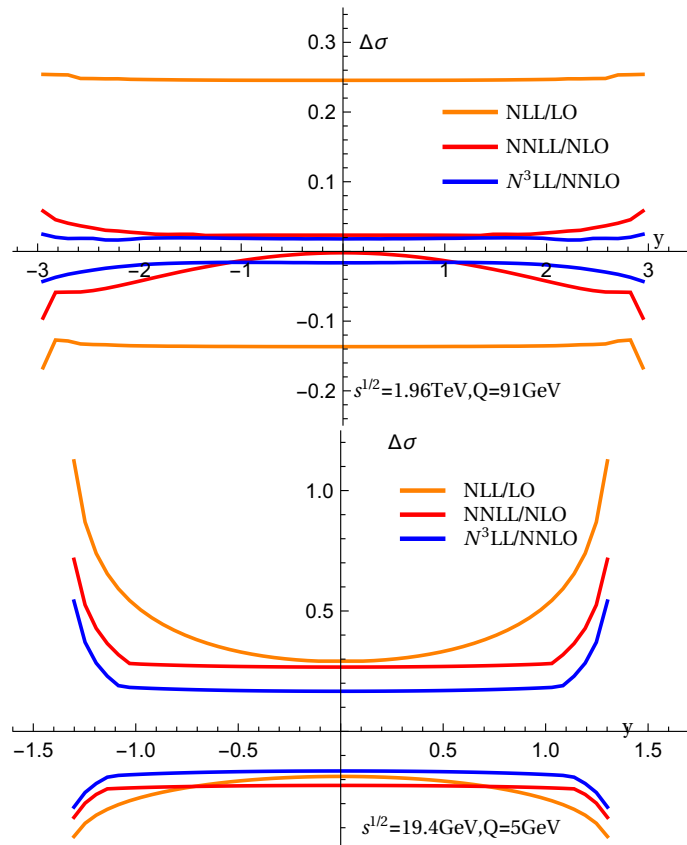


FIG. 2:  $\Delta\sigma$  for Drell-Yan process at fixed  $s$  and  $Q$  and different values of  $y$  (therefore, it scans ranges of  $x$ ). The values of  $y$  varies from maximal to minimal allowed (utmost points excluded, since cross-section is zero). Upper plot at Tevatron kinematics at Z-boson peak (experimental error  $\sim 2\%$ ). Lower plot is for one entry of E288 experiment (experimental error  $\sim 5\%$ ).

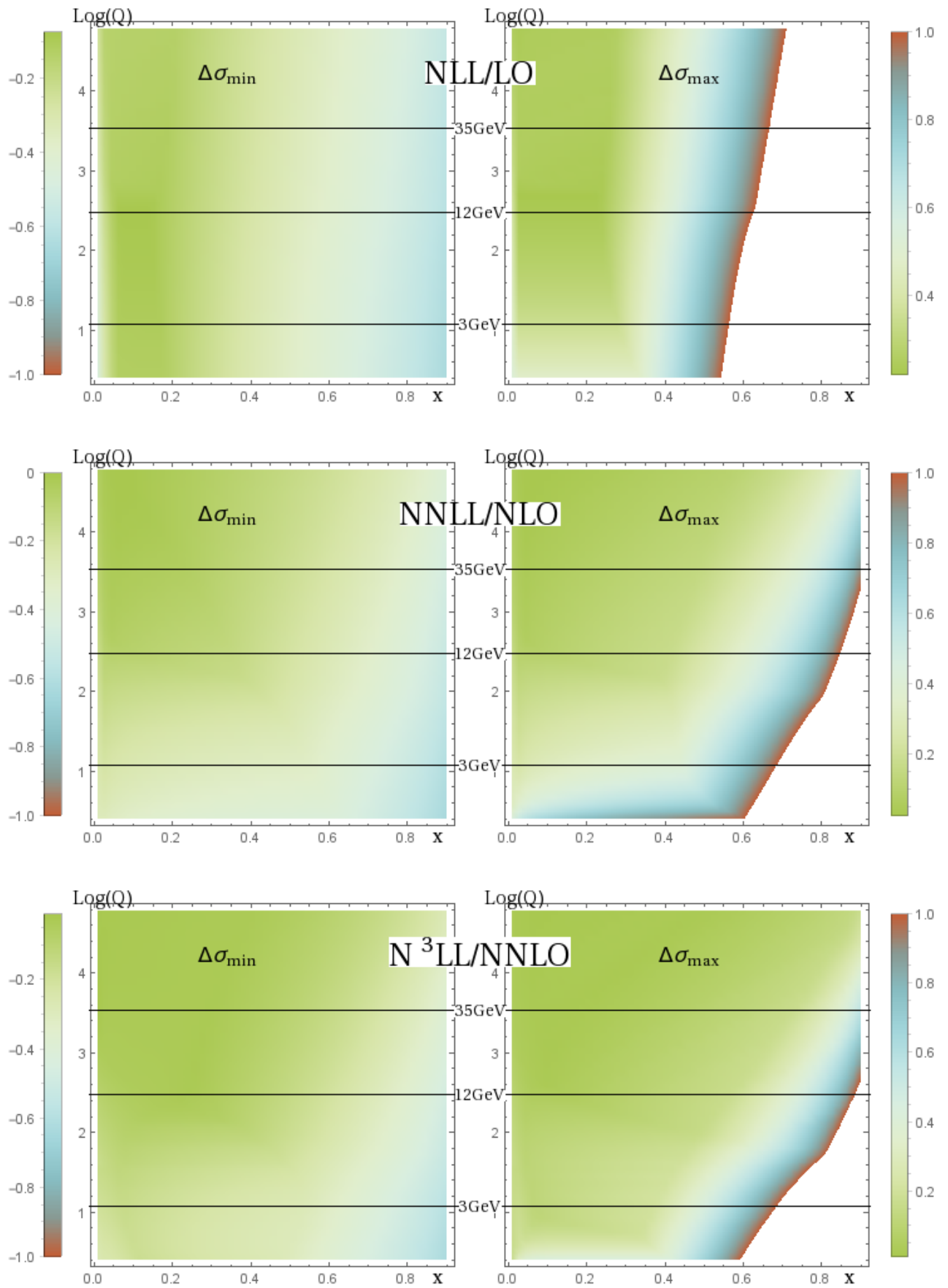


FIG. 3:  $\Delta\sigma$  for Drell-Yan process at different values of  $x$  and  $Q$  ( $y = 0$ ). The values of  $x$  varies from 0.01 to 0.9.

### III. SIDIS

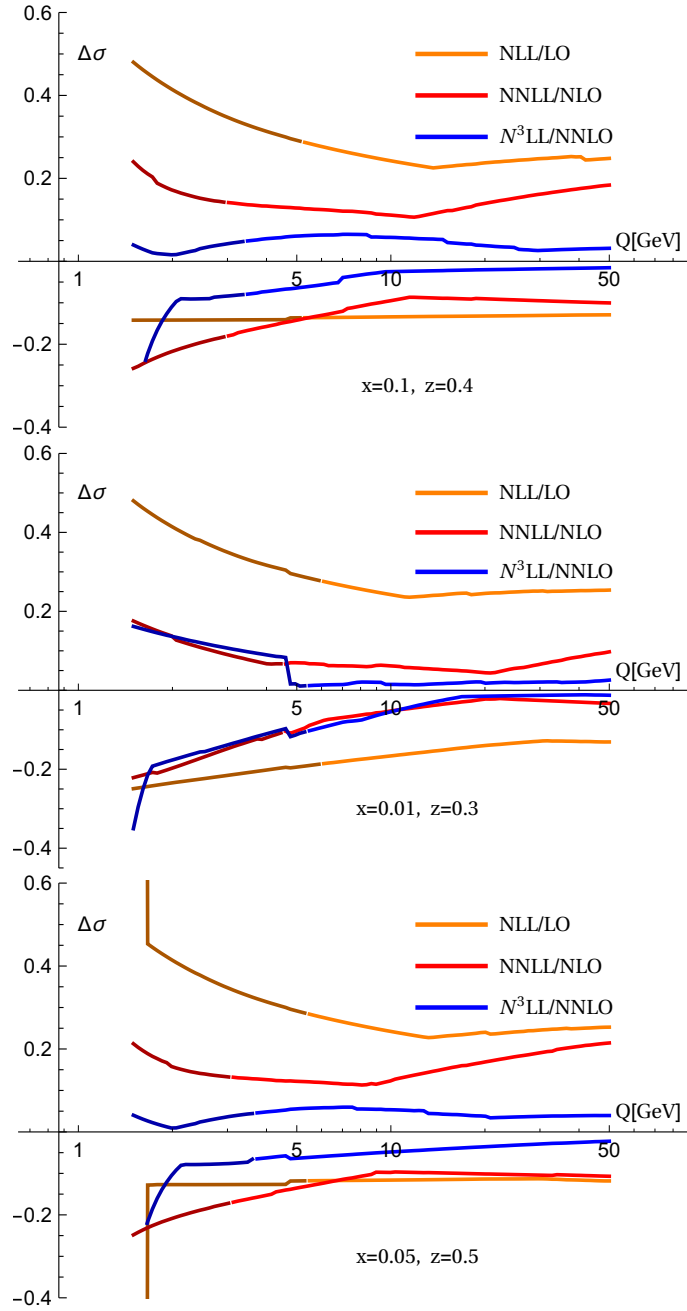


FIG. 4:  $\Delta\sigma$  for SIDIS process at fixed  $x$  and fixed  $z$  and different values of  $Q$ .  $(x, z) = (0.1, 0.4)$  presented in some HERMES bins.  $(x, z) = (0.01, 0.3)$  and  $(x, z) = (0.05, 0.5)$  presented in some COMPASS bins. **IMPORTANT:** By darker color represented the part of cross-section where the peak is away of the TMD factorization region (which we roughly estimate as  $p_T < 0.2zQ$ ).

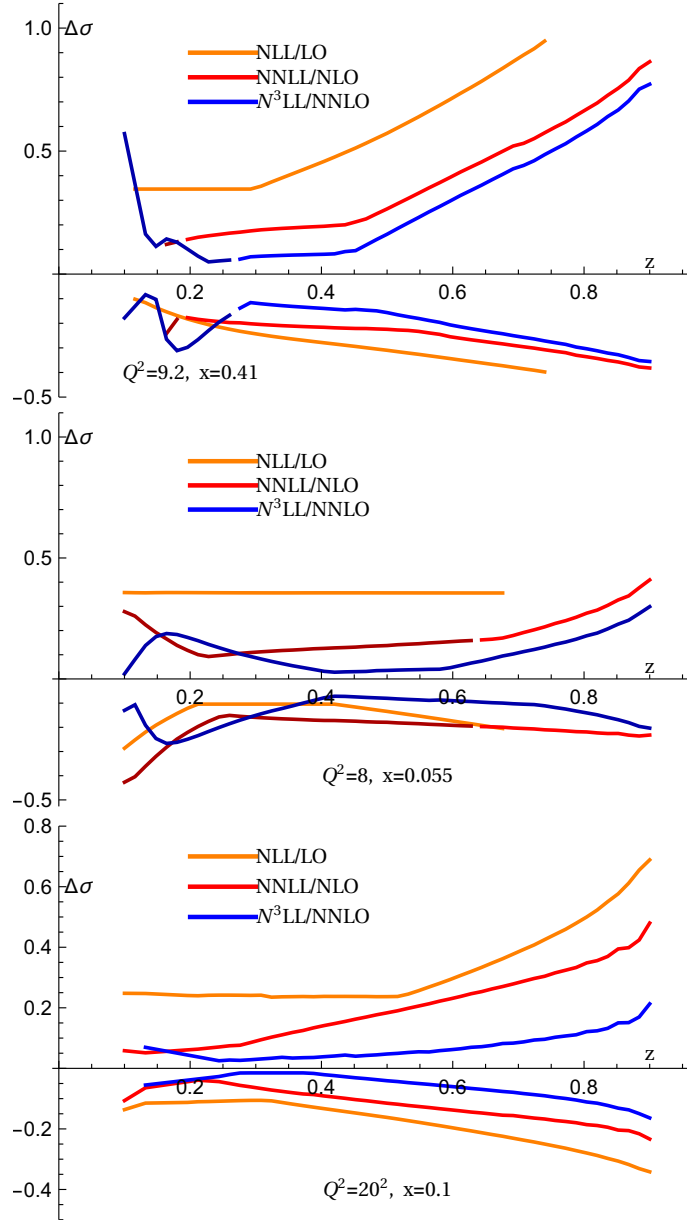


FIG. 5:  $\Delta\sigma$  for SIDIS process at fixed  $x$  and fixed  $Q$  and different values of  $z \in (0.1, 0.9)$ .  $(Q^2, x) = (9.92, 0.41)$  represent the highest bin in HERMES.  $(Q^2, x) = (8, 0.055)$  represent the highest bin in COMPASS (**IMPORTANT:** Since I do not have a proper fit of  $f_{NP}$  this is highly incorrect picture).  $(Q^2, x) = (400, 0.1)$  and  $(x, z) = (0.05, 0.5)$  represent some nice experiment.



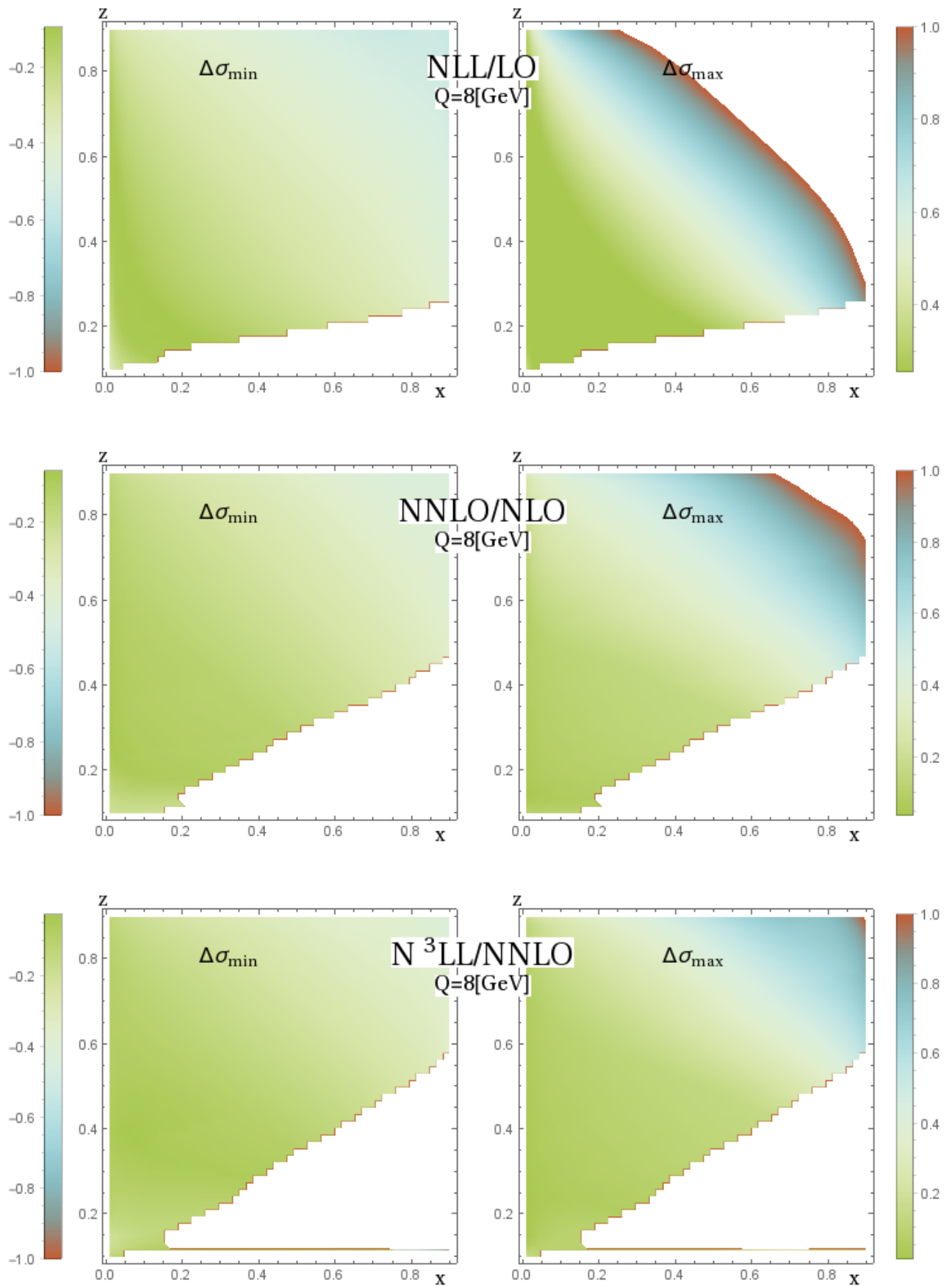


FIG. 6:  $\Delta\sigma$  for SIDIS process at different values of  $x$  and  $z$  ( $Q = 8\text{ GeV}$ ). The values of  $x$  varies from 0.01 to 0.9, values of  $z$  varies in (0.1,0.9).